Advances in Machinery, Materials Science and Engineering Application IX
M. Chen et al. (Eds.)

doi:10.3233/ATDE230453

Construction of Constitutive Model of Aeronautical Martensitic Stainless Steel 0Cr17Ni4Cu4Nb

Jilin ZHANG [a,b], Xiaoping ZHENG [c,1] and Congchao ZHAO [d]
[a] *Gansu Province Precision Machining Technology and Equipment Engineering Research Center, Lanzhou Institute of Technology, Lanzhou 730050, China*
[b] *School of Materials Science and Engineering, Lanzhou University of Technology, Lanzhou 730050, China*
[c] *College of Science, Lanzhou University of Technology, Lanzhou 730050, China*
[d] *Yuzhong County Chaoyang School, Lanzhou 730100, China*

Abstract. Aviation stainless steel 0Cr17Ni4Cu4Nb has excellent properties and is widely used in important parts of various machinery. The equivalent static compression test and impact test of 0Cr17Ni4Cu4Nb aviation Martensitic stainless steel at normal temperature were followed out by a universal test machine (UTM5305) and a high temperature separation Hopkinson test facility, respectively. The equivalent static compression data of 0.001, 0.01 and 0.1 s^{-1} at 25 °C and the dynamic stress-strain data of 25, 350, 500 and 650 °C at 25 °C and the authors got strain rates of 750, 1500, 2000, 2600, 3500 and 4500. According to them, a Johnson Cook (JC) modified constitutive model was built and its prediction accuracy was confirmed. The consequences indicate that the correlation of association (R) is 0.987513 and mean relative error (AARE) of the revised JC constitutive equation is 0.51%, which indicate that the revised JC constitutive equation is a little accurate and reliable. When they are in high strain rates, generally speaking, they can predict its stress-strain connection.

Keywords. Johnson Cook revised constitutive model, Stainless steel 0Cr17Ni4Cu4Nb

1. Introduction

The aviation stainless steel 0Cr17Ni4Cu4Nb has excellent properties and is widely used in important parts of various machinery. They will sustain hyperthermia and high tension, high rate of strain, and large impact loads in the course of working and forming stages, specifically reflected in the relationship among flow deformation stress and rate of strain, strain, and air temperature [1-2], which is the constitutive model of the material. The material has a dynamic influence on the thermal parameters during the dynamic loading process. And the aviation stainless steel 0Cr17Ni4Cu4Nb can embody this phenomenon. Especially, for finite element software, the aviation stainless

[1] Xiaoping ZHENG, Corresponding author, College of Science, Lanzhou University of Technology, Lanzhou 730050, China; E-mail: 763064753@qq.com.

steel 0Cr17Ni4Cu4Nb provides an important basis for quantitative simulation of plastic transformation of materials [3-5].

There are three major constitutive models of materials: phenomenological, physical, and artificial intelligence [6-7]. People mainly employed the Arrhenius [8] and Johnson Cook [9] models. With the rise of computer technology, artificial intelligence models are also widely used, while physical models are less widely used. The J-C constitutive model has a simple expression, clear and independent parameters, and corresponding parameters are obtained through limited experimental data, providing material parameters for finite element software simulations such as ABAQUS and LS-DYNA. Wang Yanli et al. [10] studied the dynamical mechanic performances of high nitrogen austenitic stainless steel at various air temperatures (20-600 ^{o}C) and rates of strain (100-1000 s-1), and built a Johnson Cook (JC) constitutional replica. The experimental consequences showed that the material has the sensitivities of pressure and air temperature, and the Johnson Cook (JC) constitutional model matches with the experimental results. Ding Haoxu [11] and others modified the J-C constitutive model of SUS301L-MT stainless steel based on the work heat conversion mechanism. The study indicates that the classical J-C constitutive replica cannot correctly depict the Martensite transformation strengthening effect and the adiathermic temperature rise malacia domino effect of the test steel in the course of plastic deformation at high strain rate, and the modified J-C constitutional replica can correctly describe the stress-strain relationship. Shang Bing et al. [12] used SHPB experimental equipment and hydraulic servo material testing machine (MTS) to obtain experimental data at the time of various air temperatures and rates of strain, and established a Johnson Cook example. The JC example was modified considering adiabatic temperature rise, and the modified Johnson Cook model matched well with the experimental consequences.

Therefore, in this paper, authors' research object is Martensitic stainless steel 0Cr17Ni4Cu4Nb. And authors used omnipotent testing apparatus (UTM5305) and high temperature separation Hopkinson test apparatus to conduct equivalent static compression (0.001, 0.01 and 0.1 s^{-1} at 25 ^{o}C) and impact tests (25, 350, 500 and 650 ^{o}C), and rates of strain (750, 1500, 2000, 2600, 3500 and 4500 s-1) at room temperature respectively. Then authors built a Johnson Cook (JC) modified constitutive model, contrast and analyze the precision of prediction of the replica before and after the modification, and provide theoretical and experimental basis for future cutting process determination and simulation analysis.

2. Test Materials and Methods

2.1. Testing Process

The experimental material was 0Cr17Ni4Cu4Nb stainless steel produced by Shanghai Baosteel Group Co., Ltd., which underwent solid solution treatment of heating at 1040 ^{o}C, insulation for 10-15 minutes, and air cooling. Taking into account the strain rate, temperature, and testing equipment in actual processing, the static compression test and dynamic impact test plans were 0.001, 0.01, and 0.1 s^{-1} at 25 ^{o}C, with temperatures of 25, 350, 500, and 650 ^{o}C, and strain rates of 750, 1500, 2000, 2600, 3500, and 4500 s^{-1}, respectively.

2.2. Rheological Behavior

Figure 1 and figure 2 show the real stress-strain bight relationship of stainless steel 0Cr17Ni4Cu4Nb material in the condition of equivalent statical compression and dynamical collision, respectively. From figure 1 and figure 2, it can be seen that this material owns the effects of tension reinforcing, tension rate reinforcing, and temperature weakening.

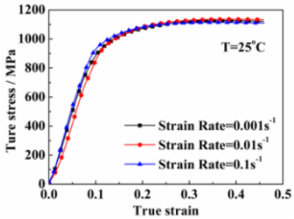

Figure 1. The true stress-strain curve of 0Cr17Ni4Cu4Nb stainless steel under quasi-static conditions.

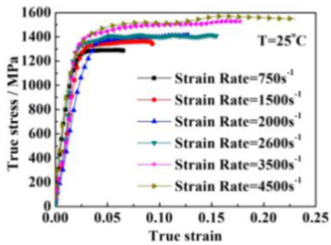

(a) T=25°C

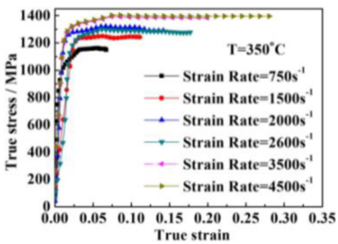

(b) T=350°C

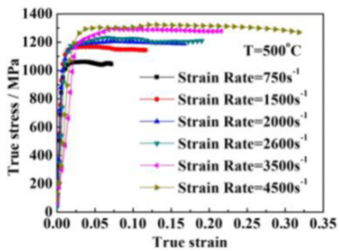

(c) T=50°C

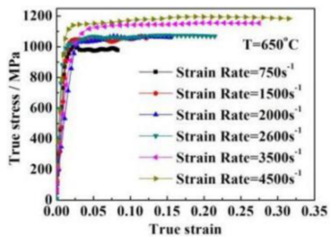

(d) T=650°C

Figure 2. True stress-strain curves of dynamic impact tests at different temperatures.

3. Establishment of Johnson-Cook (JC) Modified Constitutive Model

In the original JC constitutional replica, the three terms are multiplied and coupled with each other. When solving various parameters, they are considered to be independent of each other, without considering the matching relationship among tension, tension rate, and air temperature. In fact, cutting or stamping forming is a complex process of coupled thermal and other factors. So as to more correctly depict the dynamical automatic qualities of matters, the original JC constitutive equation must be modified to accurately guide actual production.

(1) The tension lexicon is modified to a polynomial function of strain. In quasi-static state, while its temperature is 25 °C and its strain rate is 0.01s^{-1}, the strain strengthening index of the material has a certain relationship with the tension rate and tension. When the tension and tension rate expand, they both decrease. The effect of tension rate on stress is considered in the tension rate reinforcing term, so the tension term is modified to be a polynomial of strain.

$$g(\overline{\varepsilon_{\mathrm{p}}}) = B_0 + B_1(\overline{\varepsilon_{\mathrm{p}}}) + B_2(\overline{\varepsilon_{\mathrm{p}}})^2 + B_3(\overline{\varepsilon_{\mathrm{p}}})^3 + B_4(\overline{\varepsilon_{\mathrm{p}}})^4 \tag{1}$$

(2) The tension rate term, tension rate indurating coefficient C, is changed to a binary cubic polynomial obligation of tension and tension rate. At dynamic 25 oC, the tension rate sensitiveness index of a material has the relationship with strain and strain rate. While the strain increases, the strain rate sensitivity index decreases in the field of 750 to 2600 s^{-1}, while the strain rate increases in the range of 3500 to 4500 s^{-1}, exhibiting a polynomial like behavior. Therefore, the tension rate hardening coefficient C of the tension rate term is modified to be a binary cubic polynomial obligation of tension and tension rate.

$$\begin{aligned} C = f(\dot{\varepsilon}^*, \overline{\varepsilon_{\mathrm{p}}}) &= C_0 + C_1 \ln(\dot{\varepsilon}^*) + C_2 \ln^2(\dot{\varepsilon}^*) + C_3 \ln^3(\dot{\varepsilon}^*) + C_4 \overline{\varepsilon_{\mathrm{p}}} \\ &+ C_5(\overline{\varepsilon_{\mathrm{p}}})^2 + C_6(\overline{\varepsilon_{\mathrm{p}}})^3 + C_7 \overline{\varepsilon_{\mathrm{p}}} \ln(\dot{\varepsilon}^*) + C_8 \overline{\varepsilon_{\mathrm{p}}} \ln^2(\dot{\varepsilon}^*) + C_9(\overline{\varepsilon_{\mathrm{p}}})^2 \ln(\dot{\varepsilon}^*) \end{aligned} \tag{2}$$

(3) The temperature softening index m of the temperature term is corrected to a ternary cubic polynomial obligation of tension, tension rate, and relative temperature. The third term is the temperature term, which is strictly related to strain and strain rate. Considering the mutual coupling effect, the temperature softening index m of the temperature term is modified to a ternary cubic polynomial obligation of tension, tension rate, and relative temperature.

$$\begin{aligned} m = f(\overline{\varepsilon_{\mathrm{p}}}, \dot{\varepsilon}^*, T^*) &= a_0 + a_1 \overline{\varepsilon_{\mathrm{p}}} + a_2(\overline{\varepsilon_{\mathrm{p}}})^2 + a_3(\overline{\varepsilon_{\mathrm{p}}})^3 + a_4 \ln(\dot{\varepsilon}^*) \\ &+ a_5 \ln^2(\dot{\varepsilon}^*) + a_6 \ln^3(\dot{\varepsilon}^*) + a_7 T^* + a_8(T^*)^2 + a_9(T^*)^3 + a_9 \overline{\varepsilon_{\mathrm{p}}} \dot{\varepsilon}^* T^* \end{aligned} \tag{3}$$

Based on the above discussion, the revised JC constitutive model is

$$\begin{aligned} \overline{\sigma}(\overline{\varepsilon_{\mathrm{p}}},\ \dot{\varepsilon}^*,\ T^*) &= g(\overline{\varepsilon_{\mathrm{p}}})\Gamma(\dot{\varepsilon}^*)\Theta(T^*) = g(\overline{\varepsilon_{\mathrm{p}}})(1 + C \ln \dot{\varepsilon}^*)(1 - (T^*)^m) \\ &= g(\overline{\varepsilon_{\mathrm{p}}})(1 + f(\dot{\varepsilon}^*, \overline{\varepsilon_{\mathrm{p}}}) \ln \dot{\varepsilon}^*)(1 - (T^*)^{f(\overline{\varepsilon_{\mathrm{p}}}, \dot{\varepsilon}^*, T^*)}) \end{aligned} \tag{4}$$

Among them:

$$\begin{aligned} f(\dot{\varepsilon}^*, \overline{\varepsilon_{\mathrm{p}}}) &= C_0 + C_1 \ln(\dot{\varepsilon}^*) + C_2 \ln^2(\dot{\varepsilon}^*) + C_3 \ln^3(\dot{\varepsilon}^*) + C_4 \overline{\varepsilon_{\mathrm{p}}} \\ &+ C_5(\overline{\varepsilon_{\mathrm{p}}})^2 + C_6(\overline{\varepsilon_{\mathrm{p}}})^3 + C_7 \overline{\varepsilon_{\mathrm{p}}} \ln(\dot{\varepsilon}^*) + C_8 \overline{\varepsilon_{\mathrm{p}}} \ln^2(\dot{\varepsilon}^*) + C_9(\overline{\varepsilon_{\mathrm{p}}})^2 \ln(\dot{\varepsilon}^*) \end{aligned} \tag{5}$$

$$f(\overline{\varepsilon_{\mathrm{p}}},\dot{\varepsilon}^*,T^*)=a_0+a_1\overline{\varepsilon_{\mathrm{p}}}+a_2(\overline{\varepsilon_{\mathrm{p}}})^2+a_3(\overline{\varepsilon_{\mathrm{p}}})^3+a_4\ln(\dot{\varepsilon}^*)$$
$$+a_5\ln^2(\dot{\varepsilon}^*)+a_6\ln^3(\dot{\varepsilon}^*)+a_7T^*+a_8(T^*)^2+a_9(T^*)^3+a_9\overline{\varepsilon_{\mathrm{p}}}\dot{\varepsilon}^*T^* \tag{6}$$

In the formula: $\overline{\sigma}$ is the production stress of the matter, A is the production force at the source temperature and source tension rate (quasi static), B is the tension indurating coefficient, n is the tension in indurating index, C is the tension indurating rate coefficient, m is the thermic weakening index, $\overline{\varepsilon}^{\mathrm{p}}=\varepsilon^{\mathrm{p}}/\varepsilon_0$ is the equal plastic tension, ε^{p} is the plastic strain, ε_0 is the reference strain, $\dot{\varepsilon}^*=\dot{\varepsilon}/\dot{\varepsilon}_0$ is the dimensional plastic tension rate, $\dot{\varepsilon}_0$ is the reference strain rate, $\dot{\varepsilon}$ is the plastic strain rate, T^* is the relative temperature, T_{r} is the mention temperature, T_{m} is the fusing point of the material, T is the instantaneous temperature.

3.1. Confirmation of Tension Term Parameters

Firstly, without considering the consequences of tension rate strengthening and temperature softening, the tension rate term and temperature term of the JC model are both 1, and formula (4) becomes

$$\overline{\sigma}(\overline{\varepsilon_{\mathrm{p}}})=g(\overline{\varepsilon_{\mathrm{p}}})=B_0+B_1(\overline{\varepsilon_{\mathrm{p}}})+B_2(\overline{\varepsilon_{\mathrm{p}}})^2+B_3(\overline{\varepsilon_{\mathrm{p}}})^3+B_4(\overline{\varepsilon_{\mathrm{p}}})^4 \tag{7}$$

At this point, take the reference strain $\varepsilon_0=1$, reference strain rate $\dot{\varepsilon}_0=0.01\ \mathrm{s}^{-1}$, reference temperature $T_{\mathrm{r}}=25$ ℃, and the melting point $T_{\mathrm{m}}=1420$ ℃ of the matter. Using the experiment data of temperature $T=25$ ℃ and tension rate $\dot{\varepsilon}_0=0.01\ \mathrm{s}^{-1}$ under quasi-static conditions, substitute them into formula (7) for multinomial fitting, as indicated in figure 3. The multinomial parameters B_0, B_1, B_2, B_3, and B_4 can be gotten, as displayed in table 1.

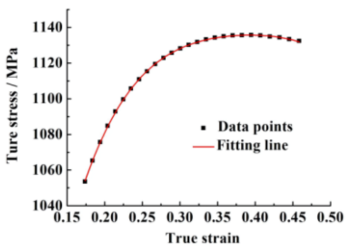

Figure 3. Strain term fitting curve.

Table 1. Strain item parameter value.

B_0	B_1	B_2	B_3	B_4
509.01581	5908.2858	-21498.54	35937.295	-23318.67

3.2. Confirmation of Tension Rate Term Parameters

Then, without considering the temperature softening effect, the temperature terms of the JC model are all 1, and formula (4) becomes

$$\bar{\sigma}(\overline{\varepsilon_{\mathrm{p}}},\ \dot{\varepsilon}^{*}) = g(\overline{\varepsilon_{\mathrm{p}}})\Gamma(\dot{\varepsilon}^{*}) = g(\overline{\varepsilon_{\mathrm{p}}})(1 + C\ln\dot{\varepsilon}^{*}) = g(\overline{\varepsilon_{\mathrm{p}}})(1 + f(\dot{\varepsilon}^{*}, \overline{\varepsilon_{\mathrm{p}}})\ln\dot{\varepsilon}^{*}) \quad (8)$$

Formula (8) is transformed into

$$\frac{\bar{\sigma}(\overline{\varepsilon_{\mathrm{p}}},\ \dot{\varepsilon}^{*})}{B_0 + B_1(\overline{\varepsilon_{\mathrm{p}}}) + B_2(\overline{\varepsilon_{\mathrm{p}}})^2 + B_3(\overline{\varepsilon_{\mathrm{p}}})^3 + B_4(\overline{\varepsilon_{\mathrm{p}}})^4} - 1 = f(\dot{\varepsilon}^{*}, \overline{\varepsilon_{\mathrm{p}}})\ln\dot{\varepsilon}^{*} \quad (9)$$

At this time, the experiment data of temperature $T = 25$ ℃ and strain rate $\dot{\varepsilon}_0 = 750\text{-}4500\,\mathrm{s}^{-1}$ under dynamic conditions are used to substitute formula (9) to calculate the value of $C = f(\dot{\varepsilon}^{*}, \overline{\varepsilon_{\mathrm{p}}})$, and regression analysis is conducted using Matlab to obtain the coefficients C_0, C_1, C_2, C_3, C_4, C_5, C_6, C_7, C_8, C_9 of binary Cubic obligation (2), as shown in table 2.

Table 2. Strain rate term parameter value.

C_0	C_1	C_2	C_3	C_4
-2.42266	0.69941	-0.06371	0.00192	-11.18017
C_5	C_6	C_7	C_8	C_9
3.04559	-9.69615	1.58625	0.18026	-0.06239

3.3. Determination of Temperature Parameters

Finally, considering the strain rate and temperature softening effects, deform formula (4) to

$$1 - \frac{\bar{\sigma}(\overline{\varepsilon_{\mathrm{p}}},\ \dot{\varepsilon}^{*},\ T^{*})}{g(\overline{\varepsilon_{\mathrm{p}}})(1 + f(\dot{\varepsilon}^{*}, \overline{\varepsilon_{\mathrm{p}}})\ln\dot{\varepsilon}^{*})} = (T^{*})^{f(\overline{\varepsilon_{\mathrm{p}}}, \dot{\varepsilon}^{*}, T^{*})} \quad (10)$$

Take the logarithm of formula (10) and deform it to obtain

$$f(\overline{\varepsilon_{\mathrm{p}}}, \dot{\varepsilon}^{*}, T^{*}) = \frac{\ln[1 - \dfrac{\bar{\sigma}(\overline{\varepsilon_{\mathrm{p}}},\ \dot{\varepsilon}^{*},\ T^{*})}{g(\overline{\varepsilon_{\mathrm{p}}})(1 + f(\dot{\varepsilon}^{*}, \overline{\varepsilon_{\mathrm{p}}})\ln\dot{\varepsilon}^{*})}]}{\ln T^{*}} \quad (11)$$

At this time, use the test data of temperature $T = 25 - 650$ ℃ and strain rate $\dot{\varepsilon}_0 = 750\text{-}4500\,\mathrm{s}^{-1}$ under dynamic conditions to calculate the value of $m = f(\overline{\varepsilon_{\mathrm{p}}}, \dot{\varepsilon}^{*}, T^{*})$ by substituting formula (11), and use Matlab for regression analysis to obtain the coefficients a_0, a_1, a_2, a_3, a_4, a_5, a_6, a_7, a_8, a_9 of the binary Cubic function (5), as shown in table 3.

Table 3. Temperature item parameter value.

a_0	a_1	a_2	a_3	a_4	a_5
-67.50836	9.61375	-118.52129	333.90202	15.06135	-1.08320
a_6	a_7	a_8	a_9	a_{10}	
0.02552	1.07963	0.00000	-3.53005	0.39414	

Therefore, the revised JC constitutive model is

$$\overline{\sigma}(\overline{\varepsilon_{\mathrm{p}}},\ \dot{\varepsilon}^*,\ T^*) = g(\overline{\varepsilon_{\mathrm{p}}})(1+f(\dot{\varepsilon}^*,\overline{\varepsilon_{\mathrm{p}}})\ln\frac{\dot{\varepsilon}}{0.01})(1-(\frac{T-25}{1395})^{f(\overline{\varepsilon_{\mathrm{p}}},\dot{\varepsilon}^*,T^*)}) \tag{12}$$

Wherein

$$g(\overline{\varepsilon_{\mathrm{p}}}) = 509.01581 + 5908.2858(\overline{\varepsilon_{\mathrm{p}}}) - 21498.54(\overline{\varepsilon_{\mathrm{p}}})^2 + 35937.295(\overline{\varepsilon_{\mathrm{p}}})^3 - 23318.67(\overline{\varepsilon_{\mathrm{p}}})^4$$

$$C = f(\dot{\varepsilon}^*,\overline{\varepsilon_{\mathrm{p}}}) = -2.42266 + 0.69941\ln(\dot{\varepsilon}^*) - 0.06371\ln^2(\dot{\varepsilon}^*) + 0.00192\ln^3(\dot{\varepsilon}^*) - 11.18017\overline{\varepsilon_{\mathrm{p}}}$$
$$+3.04559(\overline{\varepsilon_{\mathrm{p}}})^2 - 9.69615(\overline{\varepsilon_{\mathrm{p}}})^3 + 1.58625\overline{\varepsilon_{\mathrm{p}}}\ln(\dot{\varepsilon}^*) + 0.18026\overline{\varepsilon_{\mathrm{p}}}\ln^2(\dot{\varepsilon}^*) - 0.06239(\overline{\varepsilon_{\mathrm{p}}})^2\ln(\dot{\varepsilon}^*)$$

$$m = f(\overline{\varepsilon_{\mathrm{p}}},\dot{\varepsilon}^*,T^*) = -67.50836 + 9.61375\overline{\varepsilon_{\mathrm{p}}} - 118.52129(\overline{\varepsilon_{\mathrm{p}}})^2 + 333.90202(\overline{\varepsilon_{\mathrm{p}}})^3$$
$$+15.06135\ln(\dot{\varepsilon}^*) - 1.08320\ln^2(\dot{\varepsilon}^*) + 0.02552\ln^3(\dot{\varepsilon}^*) + 1.07963T^*$$
$$+0(T^*)^2 - 3.53005(T^*)^3 + 0.39414\overline{\varepsilon_{\mathrm{p}}}\dot{\varepsilon}^*T^*$$

4. Johnson-Cook (JC) Constitutive Model's Verification and Comparison before and after Modification

The stress-strain curves predicted is on the basis of the Original JC replica [13] (OJC) and the Revised JC constitutive replica (RJC), which are shown in figure 4. Further research and analysis were conducted on the accuracy of the two models using correlation coefficient (R) and mean relative fault ($AARE$). $AARE$ can reflect the compactness of experimental data and the accuracy of prediction, while R reflects the compactness of the digital relationship between data-based and anticipated values. The larger the value, the higher the compactness. They are defined as [14-15]:

$$AARE = \frac{1}{N}\sum_{i=1}^{N}\left|\frac{E_i - P_i}{E_i}\right| \tag{13}$$

$$R = \frac{\sum_{i=1}^{N}(E_i-\overline{E})(P_i-\overline{P})}{\sqrt{\sum_{i=1}^{N}(E_i-\overline{E})^2\sum_{i=1}^{N}(P_i-\overline{P})^2}} \tag{14}$$

Among them, in this research, the whole number of data is N. E_i and P_i are the true stress (MPa) of the experiment and prediction. $\overline{E}$ and $\overline{P}$ are the average values of E_i and P_i, respectively. The correlation coefficient (R) and mean relative fault ($AARE$) of the two constitutive models are indicated in figure 5 and figure 6.

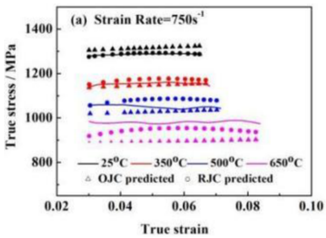

(a) $\dot{\varepsilon} = 750\ \mathrm{s}^{-1}$

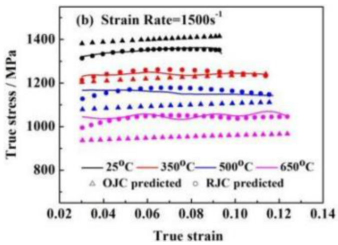

(b) $\dot{\varepsilon} = 1500\ \mathrm{s}^{-1}$

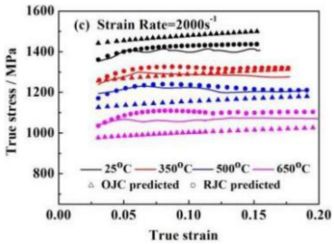

(c) $\dot{\varepsilon} = 2000\ \mathrm{s}^{-1}$

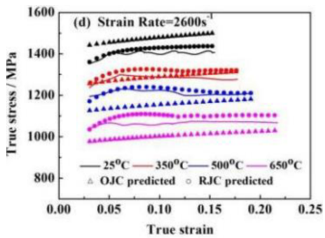

(d) $\dot{\varepsilon} = 2600\ \mathrm{s}^{-1}$

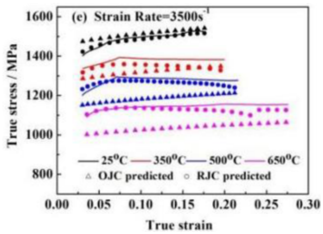

(e) $\dot{\varepsilon} = 3500\ \mathrm{s}^{-1}$

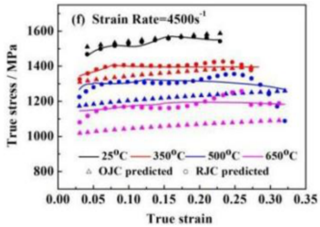

(f) $\dot{\varepsilon} = 4500\ \mathrm{s}^{-1}$

Figure 4. Comparison of True Stress Prediction and Test Values between Original JC Constitutive Model and Modified JC Constitutive Model.

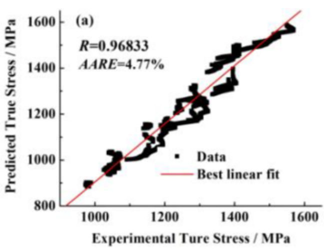

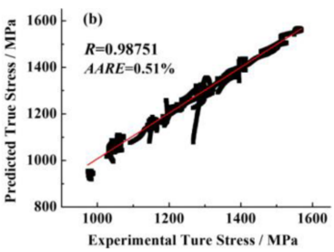

Figure 5. Relationship between original JC constitutive model, modified JC constitutive prediction value and experimental value.

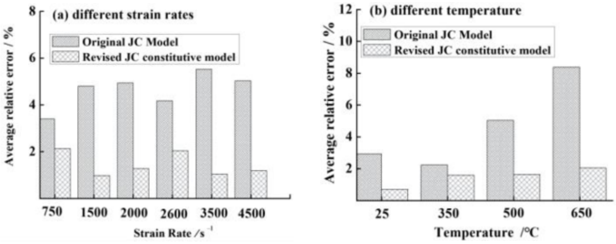

Figure 6. Comparison of the average relative errors of the original JC constitutive model and the modified JC constitutive model.

From figure 4, it can be seen that without regarding the matching relation among tension rate, strain, and air temperature, the predicted values differ from the experimental values with changes in strain rate, strain, and temperature. This article considers the coupling relationship among three factors, and the predicted curve has a highly degree of harmony with the experimental curve. From figure 5, it can be seen that the correlation coefficient (*R*) is 0.96833 and mean relative fault (*AARE*) of the original JC constitutional par is 4.77%. In this article, the correlation coefficient (*R*) is modified to be 0.987513 and average relative error (*AARE*) of the JC constitutive equation is modified to be 0.51%. Further looking in figure 6, we can see that in diverse tension rates and temperatures, the mean relative fault (*AARE*) of the original JC constitutive equation is larger than that of the modified JC constitutional par. Specifically, the maximum and minimum *AARE* of the original JC constitutive equation are 5.52% and 3.39%, respectively. A different strain rates, the maximum and minimum *AARE* of the modified JC constitutional par are 2.13% and 0.98%, respectively. By comparing the above results with figures 4-6, we can see that the modified JC constitutional par in this paper forecasts the results more accurately and is more reliable compared to the original JC constitutional par.

5. Conclusion

(1) The maximum and minimum AARE of the initial JC constitutional par are 5.52% and 3.39%, respectively. Correlation coefficients (*R*) is 0.96833 and mean relative fault (*AARE*) is 4.77%. The maximum AARE and minimum AARE of the modified JC constitutional par are 2.13% and 0.98%, respectively. The correlation coefficient (*R*) is a0.987513 and mean relative fault (*AARE*) is 0.51%. The above two replicas are near to the experimental values.

(2) Establish a revised JC constitutive model, whose predicted curve is more in line with the experimental curve, and is more accurate and reliable than the original JC constitutive model.

Acknowledgements

This work was financially backed by Key Project of Gansu Natural Science Foundation (No. 22JR5RA313), Lanzhou Talent Innovation and Entrepreneurship Project (No. 114), The first batch of Lanzhou science and technology planning projects in 2019(No. 2019-1-46),Gansu Youth Science and Technology Fund Project(No. 21JR7RA351).

References

[1] Zhang JL, Jia HS, Yi XB, et al. Effect of high temperature and high strain rate on the dynamic mechanical properties of 06Cr19Ni10 austenitic stainless steel. Iron Steel Vanadium Titanium. 2022; 43(1):145-151.

[2] Jia HS, Zhang JL, Yi XB, et al. Experimental study on rheological behavior of 022Cr18Ni14Mo2 stainless steel at high temperature and high strain rate. Journal of Mechanical Strength. 2022; 44(3): 600-606.

[3] Song Y, Garcia-Gonzalez S, Rusinek A. Constitutive models for dynamic strain aging in metals: strain rate and temperature dependences on the flow stress. Materials. 2020; 13(7): 1794-1817.

[4] Hou X, Liu ZQ, Wang B, Lv WY, Liang XL, Hua Y. Stress-strain curves and modified material constitutive model for Ti-6Al-4V over the wide ranges of strain rate and temperature. Materials. 2018; 11(6): 938-950.

[5] Zhong XZ, Yan YM, Zhang QM. Dynamic deformation behaviors and constitutive relations of high-strength Weldox700E Steel. Acta Mechanica Solida Sinica. 2019; 32(4): 431-445.

[6] Ma B, Li P, Liang Q. Comparison on high-temperature flow behavior of HNi55-7-4-2 alloy predicted by modified JC model and BP-ANN algorithm. Materials for Mechanical Engineering. 2021; 45(01):92-99.

[7] Peng XN, Guo HZ, Shi ZF, Qin C, Zhao ZL. Constitutive equations for high temperature flow stress of TC4-DT alloy incorporating strain, strain rate and temperature. Materials and Design. 2013; 50:198-206.

[8] Khan AS, Huang S. Experimental and theoretical study of mechanical behavior of 1100 aluminum in the strain rate range 10-5-104s-1. International Journal of Plasticity. 1992; 8: 397-424.

[9] Lin YC, Chen XM. A critical review of experimental results and constitutive descriptions for metals and alloys in hot working. Materials & Design. 2011; 32(4):1733-1759.

[10] Wang YL, Jia GZ, Zhang T, Wang MM, Ji W, Mu XM. Dynamic mechanical behaviors of high-nitrogen austenitic stainless steel under high temperature and its constitutive model. Explosion and Shock Waves. 2018; 38(4): 834-840.

[11] Ding HX, Zhu T, Xiao SN, Wang XR, Yang YW, Yang B. Modified J-C constitutive model of SUS301L-MT stainless steel based on work-heat conversion mechanism. Materials for Mechanical Engineering. 2022; 46(01):97-103+110.

[12] Shang B, Sheng J, Wang BZ, Hu SS. Dynamic mechanical properties and constitutive model of stainless steel materials. Explosion and Shock. 2008; 28(6):527-531.

[13] Zhang JL, Jia HS, Yi XB, et al. Dynamic mechanical properties and comparison of two constitutive models for martensitic stainless steel 0Cr17Ni4Cu4Nb. Materials Research Express. 2021; 8(10):106501.

[14] Niu DX, Zhao C, Li DX, et al. Constitutive modeling of the flow stress behavior for the hot deformation of Cu-15Ni-8Sn alloys. Frontiers in Materials. 2022; 7(12):577867.

[15] Ma B, Li P, Liang Q. Comparison on high-temperature flow behavior of HNi55-7-4-2 alloy predicted by modified JC model and BP-ANN algorithm. Chinese Journal of Materials Research. 2021; 45(1):92-99.